Property-Optimized Gaussian Basis Sets for Lanthanides

Dmitrij Rappoport[a]

Department of Chemistry, University of California, Irvine, CA 92697,

USA

(Dated: 3 August 2021)

Property-optimized Gaussian basis sets of split-valence, triple-zeta and quadruple-zeta valence quality are developed for the lanthanides Ce–Lu for use with small-core relativistic effective core potentials. They are constructed in a systematic fashion by augmenting def2 orbital basis sets with diffuse basis functions and minimizing negative static isotropic polarizabilities of lanthanide atoms with respect to basis set exponents within the unrestricted Hartree–Fock method. The basis set quality is assessed using a test set of 70 molecules containing the lanthanides in their common oxidation states and f electron occupations. 5d orbital occupation turns out to be the determining factor for the basis set convergence of polarizabilities in lanthanide atoms and the molecular test set. Therefore, two series of property-optimized basis sets are defined. The augmented def2-SVPD, def2-TZVPPD, and def2-QZVPPD basis sets balance the accuracy of polarizabilities across lanthanide oxidation states. The relative errors in atomic and molecular polarizability calculations are $\leq 8\%$ for augmented split-valence basis sets, $\leq 2.5\%$ for augmented triple-zeta valence basis sets, and $\leq 1\%$ for augmented quadruple-zeta valence basis sets. In addition, extended def2-TZVPPDD and def2-QZVPPDD are provided for accurate calculations of lanthanide atoms and neutral clusters. The property-optimized basis sets developed in this work are shown to accurately reproduce electronic absorption spectra of a series of $LnCp'^-_3$ complexes ($Cp' = C_5H_4SiMe_3$, Ln = Ce–Nd, Sm) with time-dependent density functional theory.

---

[a]Electronic mail: dmitrij@rappoport.org

I. INTRODUCTION

Lanthanides show a wealth of optical, magnetic, and chemical behaviors due to the presence of partially filled 5d and 4f subshells. The electronic ground states of lanthanide atoms span the range from closed-shell singlet (Yb ^1S) to nonet (Gd $^9D°$).[1,2] The many low-lying excited states, multireference character, and relativistic effects add further complexity to their electronic structures.[3–5] Both relativistic all-electron methods and effective core potential (ECP) methods are popular in quantum chemical modeling of lanthanide-containing compounds, each having their own atomic basis set requirements. The development of Gaussian basis sets for lanthanides and actinides has been recently reviewed.[6–8] All-electron Gaussian basis sets for lanthanides include third-order Douglas–Kroll (DK3) basis sets of Hirao and co-workers,[9,10] ANO-RCC basis sets,[11] SARC basis sets,[12,13] the segmented–contracted DKH basis set by Dolg,[14] Sapporo-DK-nZP,[15] cc-pVnZ basis sets,[6,16] and DZP and TZP basis sets by Jorge and co-workers.[17–19] The relativistic basis set family of Dyall and co-workers was developed for four-component Dirac–Hartree–Fock calculations.[20] More recently, the ANO-R basis sets[21] and Karlsruhe x2c basis sets[22,23] were optimized for the exact two-component (x2c) method. Among ECP approaches, Gaussian basis sets are available for large-core ECPs, which include the 4f subshell in the atomic core,[24–27] and small-core ECPs, which allow for varying 4f configurations.[28–30] The def2 series of segmented contracted basis sets[31] has been extended to the elements Ce–Lu by Weigend and co-workers[7,30] for use with small-core ECPs of the Wood–Boring type.[32]

With orbital basis sets designed to accurately reproduce ground-state wavefunctions, the dominant source of errors in calculations of response properties with these basis sets is the lack of low-exponent (diffuse) basis functions.[33–35] Diffuse basis functions have little influence on the ground-state energies but are crucial for representing the orbital response to external perturbations. At present, diffuse augmentation for lanthanides is rare in the literature. Diffuse basis functions were reported for selected lanthanides by Buchachenko and co-workers.[36] Sekiya and co-workers obtained diffuse augmentation for their basis sets by downward extrapolation.[15] Jorge and co-workers developed augmented basis sets from energy optimizations of atomic anions.[18,19] The latter two approaches tend to produce extensive augmentation and small diffuse basis set exponents, which impact the efficiency of integral-direct methods and can cause numerical stability problems.

The construction of property-optimized basis sets derives from the variational property of static polarizabilities.[37] Diffuse augmentation of property-optimized basis sets is obtained by minimizing a target quantity, namely the negative static Hartree–Fock (HF) polarizability, with respect to basis set parameters. The basis set optimization procedure is equivalent to that for energy-optimized orbital basis sets, in which the ground-state HF energy is typically the target quantity.[30,31,33–35] As we previously reported,[37] the bulk of the basis set errors in static polarizabilities is addressed by adding only few diffuse basis functions with optimized exponents. The differential contributions of a second, third, etc., sets of basis functions with the same angular momentum (l) quantum number and optimized exponents decrease exponentially, making multiple augmentation usually unnecessary. We also found that the diffuse augmentation in these basis sets does not need to increase with the size of the underlying orbital basis set.

This paper reports property-optimized augmented Gaussian basis sets of split-valence, triple-zeta and quadruple-zeta valence quality for the elements Ce–Lu. The diffuse augmentation is obtained by minimizing negative static HF polarizabilities of the Ce–Lu atoms in their $4f^n 5d^1$ ($n = 1 - 14$) and $4f^{n+1}$ ($n = 2 - 13$) configurations. We assess the accuracy of the property-optimized basis sets using an extended version of the molecular test set of Weigend and co-workers, which includes common oxidation states of the lanthanides.[7,30] Our construction of property-optimized basis sets aims for $\leq 8\%$ target accuracy for augmented split-valence basis sets, $\leq 2.5\%$ for augmented triple-zeta valence basis sets, slightly relaxed from the target of $\leq 2\%$ used in our previous work, and $\leq 1\%$ for augmented quadruple-zeta valence basis sets. However, the selection of diffuse augmentations for the lanthanides is complicated by the strong and somewhat unexpected sensitivity of the basis set requirements in lanthanides to their oxidation states and 5d occupations. In order to balance accuracy and basis set size, we define two series of property-optimized augmented basis sets for Ce–Lu. The def2-SVPD, def2-TZVPPD, and def2-QZVPPD basis sets provide economic augmentation and balance the accuracy of polarizabilities across lanthanide oxidation states. In addition, the def2-TZVPPDD and def2-QZVPPDD include larger diffuse sets and are only needed for accurate calculations of lanthanide atoms and neutral clusters.

This paper is structured as follows. We briefly describe the optimization procedure for property-optimized basis sets in Section II. The resulting basis sets and their basis set convergence are discussed in Section III. The use of property-optimized basis sets is illus-

trated in Section IV for electronic absorption spectra of a series of $LnCp_3'^-$ complexes (Cp' = $C_5H_4SiMe_3$, Ln = Ce–Nd Sm).[38–40] We close with a discussion in Section V and present our conclusions in Section VI.

II. METHODS

The construction of property-optimized basis sets is described in Ref. 37, to which we refer for details. Only a brief discussion will be given here. The basis set optimization procedure relies on the variational property of static polarizabilities. Specifically, the negative mn component of the static polarizability, $-\alpha^{mn}$ ($m, n = x, y, z$), is the stationary point of the Hylleraas functional[41,42]

$$G[\tilde{\Psi}^m, \tilde{\Psi}^n] = \langle \tilde{\Psi}^m|(H^{(0)} - E^{(0)})|\tilde{\Psi}^n\rangle + \langle \tilde{\Psi}^m|H^n|\Psi^{(0)}\rangle + \langle \Psi^{(0)}|H^m|\tilde{\Psi}^n\rangle, \tag{1}$$

where $|\Psi^{(0)}\rangle$ is an eigenfunction of the unperturbed Hamiltonian $H^{(0)}$ with the corresponding energy eigenvalue $E^{(0)}$, and the operators H^m, H^n are the m and n components of the electric dipole perturbation. If the functional $G[\tilde{\Psi}^m, \tilde{\Psi}^n]$ is a positive definite bilinear form, which is the case when $|\Psi^{(0)}\rangle$ is the ground state of the Hamiltonian $H^{(0)}$ (or the lowest-energy state within a given symmetry representation), then the stationary point is a minimum,

$$G[\tilde{\Psi}^m, \tilde{\Psi}^n] \geq G[\Psi^m, \Psi^n] = -\alpha^{mn}, \tag{2}$$

where $|\Psi^m\rangle$ and $|\Psi^n\rangle$ correspond to the first-order wavefunction response to the dipole perturbations H^m and H^n, respectively. This variational condition allows us to obtain property-optimized basis sets by minimizing negative static polarizabilities with respect to basis set parameters. As in our previous work,[37] the basis set optimization procedure utilizes the static isotropic polarizabilities $\alpha_{\text{iso}} = \frac{1}{3} \sum_{m=x,y,z} \alpha^{mm}$ of lanthanide atoms within the unrestricted HF (UHF) method.

We note that the Hylleraas functional is not variational with respect to the unperturbed electronic state. The strict application of the minimum property of Eq. 2 thus requires that the basis set is held constant in ground-state UHF calculations and that dual-basis techniques are used for computing polarizabilities.[43,44] Indeed, excessive diffuse augmentation leads to an admixture of excited electronic states to the basis set representation of the ground-state wavefunction, which has a negligible effect on energies but presents itself as overpolariza-

tion.[45] However, we find that this issue rarely presents problems in property-optimized basis sets with moderate diffuse augmentation.

The reference UHF states of the atoms Ce–Lu with def2-SVP basis sets[30] and small-core ECPs[32] were determined by exhaustive search over atomic orbital (AO) occupations in D_{2h} symmetry. AO occupations corresponding to the $4f^n 5d^1$ configuration were obtained for Ce–Sm, Gd–Tm, Lu ($n = 1$–6, 8–12, 14). Reference states corresponding to the $4f^{n+1}$ configuration were determined for Pr–Eu, Tb–Yb ($n = 2$–6, 8–13). The AO occupations and UHF energies of the reference states are given in the Section S1 of the Supplementary Material (SM).

In the construction of the property-optimized basis sets for the lanthanides, the def2-SVP, def2-TZVPP, and def2-QZVPP orbital basis sets[30] were successively augmented with uncontracted diffuse basis functions with $l = 0 - 4$ (s, p, d, f, g) angular momentum quantum numbers. The static UHF polarizabilities were evaluated using nonorthonormal Krylov-space methods[46] with 10^{-10} convergence threshold for the residual norm. The exponents of the diffuse basis functions were optimized for each augmentation pattern by minimizing the negative logarithmic UHF polarizabilities ($-\log \alpha_{\mathrm{iso}}$) of the atoms. The convergence criteria for the basis set optimization were 10^{-8} a.u. for ($-\log \alpha_{\mathrm{iso}}$) and 10^{-5} a.u. for its gradient. The polarizability derivatives with respect to basis set parameters were evaluated numerically using a 4-point central difference formula with 10^{-4} a.u. spacing. In the following we use a compact notation to describe diffuse augmentation. A 1p diffuse set, for example, denotes a complete set of diffuse basis functions with angular momentum quantum number $l = 1$ (p). The basis set limit in atomic calculations was approximated by def2-QZVPP basis including 2s2p2d2f2g augmentation from even-tempered downward extrapolation.

Since the minimum property of the Hylleraas functional $G[\tilde{\Psi}^m, \tilde{\Psi}^n]$ relies on the reference state $|\Psi^{(0)}\rangle$ being stable,[47–49] the optimization procedure fails in the presence of reference state instabilities. We observed electronic instabilities with UHF for the Tm $4f^{12}5d^1$ and Lu $4f^{14}5d^1$ reference states, which could not be remedied by symmetry breaking. The basis set optimization procedure fails in these cases. In the Tm $4f^{12}5d^1$ reference state, the basis set exponents were determined by extrapolation from Ce–Sm, Gd–Er $4f^n 5d^1$ ($n = 1 - 11$) states, while basis set optimizations for the Lu $4f^{14}5d^1$ succeeded with 1f diffuse augmentation. See Section III for details.

The molecular test set of Weigend and co-workers[30] was extended in this work to 70

molecules covering the elements Ce–Lu in their common oxidation states and f electron occupations. The dioxides CeO_2 and TbO_2 were included as representatives of the +4 oxidation state. The set of lanthanide dimers was extended by the early-lanthanide molecules Ce_2 and Pr_2. Several additions were made to obtain complete coverage of the low-valent states of Tb, Ho, Er as well as Pm, Eu, Tb, Tm, Yb +3 oxidation states. For consistency with Ref. 30, the structures of the added molecules were optimized by density functional theory (DFT) with the BP86 exchange–correlation functional,[50,51] the Cao–Dolg basis sets[29] for the lanthanides, and def2-QZVP basis sets[52] for all other atoms. The structures of some molecules in the test set were symmetrized and re-optimized based on the available literature data. The orbital occupations, spin expectation values, and UHF energies of the extended molecular test set are given in the Section S3 of the SM. 5d and 4f orbital occupations from natural population analysis[53] are also included. The Cartesian coordinates of the optimized molecular structures are provided in the Section S5 of the SM. Calculations with def2-QZVPP basis sets and 1s1p1d1f1g extrapolated augmentations for all elements (1s1p1d1f for H) were used to approximate the basis set limits of molecular polarizabilities. All calculations were performed with the Turbomole program package, version 7.5.[54,55]

III. RESULTS

The competition between the 4f and 5d subshells is a characteristic feature of lanthanides. The experimental ground states of the elements Ce, Gd, and Lu have $4f^n5d^1$ configurations ($n = 1, 7, 14$). The elements Pr–Eu and Tb–Yb have the ground state configurations $4f^{n+1}$ with $n = 2$–6, 8–13, however, with the exceptions of Eu and Yb, the corresponding $4f^n5d^1$ configurations are close in energy. The atomic states arising from $4f^n5d^1$ and $4f^{n+1}$ configurations show drastically different convergence of their static isotropic polarizabilities α_{iso}, as illustrated in Fig. 1 for the Pr atom. The polarizability of the Pr $4f^3$ state is ca. 11% away from the basis set limit with the unaugmented def2-SVP and def2-TZVPP basis sets and is still 4% in error with the def2-QZVPP basis set, see Fig. 1(a). However, the basis set limit is reached with the addition of a 1p diffuse set, with all augmented basis sets having less than 1% relative error. This is line with our previous results for the neighboring elements Ba and La, which converge quickly to the basis set limit and require at most 1p diffuse augmentation.[37]
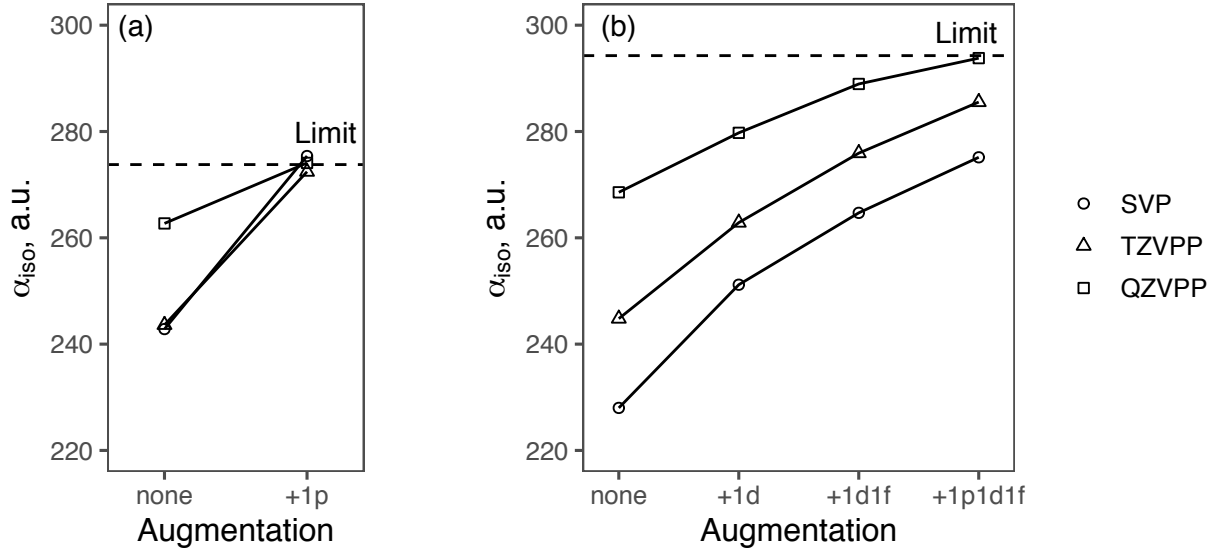
6

FIG. 1. Basis set convergence of static isotropic HF polarizability α_{iso} of the Pr atom with diffuse augmentation using optimized exponents in the (a) $4f^3$ and (b) $4f^25d^1$ states. Horizontal dashed lines represent the basis set limits.

By contrast, the Pr $4f^25d^1$ state shows very slow convergence to the basis set limit, see Fig. 1(b). The def2-SVP basis set has a 22.5% relative error compared to the basis set limit, while the def2-QZVPP basis set still 8.7% away from the limit. The largest contributions to the polarizability of the Pr $4f^25d^1$ state are, in decreasing order, from 1d, 1f, and 1p diffuse sets. The 1p1d1f augmented double-zeta, triple-zeta valence, and quadruple-zeta valence basis sets have 6.5%, 3.0%, and 0.2% relative errors, respectively. These trends continue throughout the lanthanide series, as shown in the Section S2 of the SM. The polarizabilities of $4f^{n+1}$ states convergence quickly towards the basis set limit, similar to that of Ba and La. The unaugmented basis sets already yield relatively small basis set errors, while the addition of a 1p diffuse set is sufficient to reach the basis set limit. The $4f^n5d^1$ states are much more problematic. As a consequence of the 5d occupation, diffuse d and f functions are required to accurately capture the orbital response in these states. The largest basis set errors are observed in the early lanthanides Ce–Nd, in which 5d orbitals have the largest spatial extent due to lanthanide contraction.[6]

The construction of the def2-SVP basis sets for lanthanides by removing one basis function each from the p, d, and f spaces and re-optimizing[30] produces a gap in p basis set exponents in some lanthanide atoms. For Ce–Nd and Ho, the ratios between the smallest and the second-

smallest p function exponents in their def2-SVP basis are greater than 5. The unconstrained optimization of def2-SVP basis sets for lanthanides (except for Pr, Eu, Yb) and def2-TZVPP basis sets of Nd, Sm, Tb–Er with 1p augmentation thus causes the p basis function exponents to intrude into the valence/polarization space. In these cases, the diffuse p basis function exponents were fixed to $\frac{1}{2}\zeta_{p,\mathrm{min}}$, where $\zeta_{p,\mathrm{min}}$ is the smallest p function exponent of the orbital basis set. Additionally, we investigated the effect of inserting a 1p polarization set into def2-SVP and def2-TZVPP basis sets with exponents obtained by interpolation. The results are included in the Section S1 of the SM. The addition of the 1p polarization set accelerates the convergence of atomic polarizabilities with augmented def2-SVP and def2-TZVPP basis sets but was found to have only a modest effect in the molecular test set. This avenue was not further pursued in this work.

The Tm $4f^{12}5d^1$ and Lu $4f^{14}5d^1$ states pose a different set of issues due to electronic instabilities in their UHF wavefunctions. The instability of the Tm $4f^{12}5d^1$ state shows up in the very large polarizabilities with augmented basis sets, which far exceed those of the neighboring elements Er and Yb, see Section S2 of the SM. Moreover, the addition of diffuse f basis functions leads to negative static polarizability components. We note that all electronic states corresponding to the Tm $4f^{12}5d^1$ configuration were enumerated and shown to suffer from the instabilities described here. The exponents of the diffuse basis functions for Tm were thus obtained by extrapolation from optimized Ce–Sm, Gd–Er basis sets. In Lu $4f^{14}5d^1$ states, the static polarizability components turn negative with def2-TZVPP and def2-QZVPP basis sets. The addition of 1f diffuse sets removes the instabilities, while basis functions with other l quantum numbers do not seem to have an appreciable effect on the polarizability. However, the basis set convergence of the polarizability of the Lu $4f^{14}5d^1$ state is not monotonic and the corresponding basis set error estimates are not reliable.

Given that $4f^n5d^1$ configurations correspond to excited states in lanthanide atoms (except Ce, Gd, and Lu) and that the occupation of diffuse 5d orbitals leads to slow basis set convergence of response properties, it might be tempting to leave these states out from the construction of property-optimized basis sets. 5d orbital occupation is not limited to neutral lanthanide atoms, however. On the contrary, 5d orbitals are occupied in lanthanide clusters[56–59] and contribute to bonding in low-valent small molecules[4,60,61] and a growing number of organometallic complexes[40,62–67] of lanthanides. In selecting the augmentation patterns for the property-optimized basis sets, we have to take into consideration the basis

set convergence in both $4f^n5d^1$ atomic states (Ce–Sm, Gd–Tm, Lu, $n = 1$–6, 8–12, 14) and $4f^{n+1}$ atomic states (Pr–Eu, Tb–Yb, $n = 2$–6, 8–13) as well as in the molecular test. The molecular test set results display a large variation across the lanthanide series and as a function of the lanthanide oxidation state. We aim for a target accuracy of $\leq 8\%$ for augmented split-valence basis sets, $\leq 2.5\%$ for augmented triple-zeta valence basis sets, and $\leq 1\%$ for augmented quadruple-zeta valence basis sets. We give a brief summary of the trends in the molecular test set in the following. The complete molecular test results are compiled in the Section S4 of the SM.

a. Ce–Pr The neutral dimers Ce_2 and Pr_2 are derived from the $4f^{n-1}5d^2$ atomic states $(n = 1$–2)[56–59,68] and show similarly slow basis set convergence to the $4f^n5d^1$ states of the neutral atoms. 1p1d1f diffuse augmentation is necessary to reach the target accuracy. The example of Pr_2 also illustrates the importance of balancing the contributions from diffuse basis functions of different l quantum numbers. def2-SVP basis sets with the Pr $4f^3$ state–based 1p diffuse augmentation overestimate the basis set limit in Pr_2 by 15%, while the Pr $4f^25d^1$-based 1p1d1f augmentation yields an error of only 1.8%. Low-valent Ce and Pr compounds with lanthanide atoms in the +1 and +2 oxidation states show faster basis set convergence than the neutral lanthanide dimers due to only partial 5d occupations. 1d1f diffuse augmentation is generally sufficient to achieve target accuracy, while the effect of diffuse p functions is negligible in divalent compounds. The compounds of Ce and Pr in their most common +3 oxidation state are highly ionic and contain Ln^{+3} cations with $4f^n$ configurations $(n = 1$–2).[69–72] These compounds behave similarly to alkali and earth alkali metal salts, in which the basis set convergence of polarizabilities is dominated by the negatively charged counterions, while diffuse augmentation on the metal atoms has essentially no effect.[37] Likewise, diffuse augmentation of the Ce atom in CeO_2 (oxidation state +4) contributes only little to its polarizability.

b. Nd–Sm Compared to Ce–Pr, the basis set requirements of the following elements Nd–Sm are reduced due to their more compact valence orbitals.[1,6] In particular, diffuse p and f basis functions make relatively small contributions to polarizabilities in low-valent compounds of these elements. The diffuse augmentations optimized using $4f^{n+1}$ reference states $(n = 3$–5) are thus unsuitable for molecular calculations. 1d augmented basis sets (optimized using $4f^n5d^1$ reference states, $n = 3$–5) give on average the desired accuracy. Within this average, however, the effect of diffuse 1d augmentation decreases considerably

9

with the lanthanide oxidation state. The compounds of Nd–Sm in their +1 and +2 oxidation states reach the target accuracy with 1d diffuse augmentation, while the ionic trivalent compounds require no diffuse augmentation at all on the lanthanide atoms.

c. Eu, Yb Due to the presence of half-filled or completely filled 4f shells, Eu and Yb have the highest 4f→5d promotion energies of the lanthanide series.[1] Because 5d orbitals are unoccupied in Eu and Yb compounds, we observe rapid basis set convergence, in line with that of Ba and La compounds.[37] Similar to the earth alkali dimers, the Eu_2 and Yb_2 molecules are predominantly van der Waals bound.[56,73,74] The effect of 1p diffuse augmentation in Eu and Yb compounds is only noticeable when def2-TZVPP and def2-QZVPP basis sets are used and higher accuracy is desired. The ionic compounds of Eu and Yb in +2 and +3 oxidation states do not require diffuse augmentation on the lanthanide atoms.

d. Gd–Ho The basis set convergence in compounds of Gd–Ho is similar to that in Nd–Sm. The neutral dimer Gd_2 is characterized by very slow basis set convergence and requires 1p1d1f diffuse augmentation to reach target accuracy. However, the compounds of Gd–Ho in positive oxidation states are well described using 1d diffuse augmentation. The trihalides of Gd–Ho require no diffuse augmentation on the lanthanide atoms at all. TbO_2 contains Tb in the oxidation state +4 and shows rapid basis set convergence, apart from the anomalous behavior of augmented def2-SVP basis sets, which significantly overestimate its polarizability.

e. Er–Tm The compounds of the late lanthanides Er–Tm show the fastest basis set convergence of the lanthanide-containing molecules with 5d occupations. Like many other trends in the basis set requirements of lanthanides, this effect can be attributed to the lanthanide contraction, which reduces the spatial extent of 5d orbitals in these elements. 1d diffuse augmentation achieves the target accuracy on average for the molecules containing Er–Tm.

f. Lu The properties of Lu set it apart from the other lanthanides and are subject to a protracted debate about whether it should even be included in the lanthanide series.[75] With respect to the basis set convergence, the Lu $4f^{14}5d^1$ state is distinct from the other $4f^n5d^1$ atomic states of lanthanides and requires 1f diffuse augmentation. Lu also differs from the neighboring elements Hf and Nb, which, like other transition metals, depend on 1p diffuse augmentation.[37] The instabilities of the Lu $4f^{14}5d^1$ state with UHF make the basis set convergence difficult to quantify, as discussed above. However, the polarizabilities of Lu

compounds are within target accuracy without diffuse augmentation on the Lu atom, with the exception of the Lu_2 dimer, which reaches the target accuracy with 1f augmentation.

The large variation in the augmentation requirements in lanthanide atoms and lanthanide-containing molecules leads us to deviate from the scheme we developed in our previous work for the main-group elements and transition metals and to define two series of property-optimized augmented basis sets for Ce–Lu. The generally recommended def2-SVPD, def2-TZVPPD, and def2-QZVPPD basis sets are designed for calculations of compounds containing lanthanides in positive oxidation states. They are constructed to yield the target accuracy on average across the molecular test set. In addition, we define extended def2-TZVPPDD and def2-QZVPPDD basis sets, which are suitable for accurate studies of lanthanide atoms and neutral clusters and yield the target accuracy specifically for lanthanide atoms in $4f^n5d^1$ and $4f^{n+1}$ atomic states and in neutral metal dimers. The augmentation patterns of the property-optimized basis sets are shown in Table I. The statistics of relative errors of static isotropic UHF polarizabilities are presented in Table II for the atoms Ce–Yb in their $4f^n5d^1$ and $4f^{n+1}$ states (except Tm $4f^{12}5d^1$). The relative errors of static isotropic UHF polarizabilities of the molecular test set are shown in Table III. Fig. 2 summarizes the molecular test results by lanthanide oxidation state. See Section S2 of the SM for the complete data.

The default augmented basis sets def2-SVPD, def2-TZVPPD, and def2-QZVPPD are designed for all lanthanide calculations except in atoms and neutral metal clusters. These basis sets contain 1d1f diffuse augmentation for Ce and Pr and 1d augmentation for the later lanthanides Nd–Sm, Gd–Tm. As in our previous work,[37] the diffuse set does not increase with the size of the underlying basis set. For Eu and Yb, diffuse augmentation is only added to the def2-QZVPP basis sets in order to obtain the target accuracy of $\leq 1\%$ basis set error. No augmentation is included in the Lu basis sets. The mean unsigned error (MUE) with the def2-SVPD basis sets is 8.0% for the atomic polarizabilities and 4.4% for the molecular test set relative to the basis set limit, compared to 12.2% MUE for atomic calculations and 22.6% MUE for the molecular test set using the unaugmented def2-SVP basis sets, see Tables II and III. With the def2-TZVPPD and def2-QZVPPD basis sets, the MUEs for the molecular test set are 1.9% and 0.9%, respectively.

Fig. 2 offers a more detailed view of the relative errors of static isotropic UHF polarizabilities within the molecular test set by oxidation state using box-and-whiskers plots. The

11

median error within each group is shown by a thick horizontal line, while the box covers the range between the first and third quartiles (interquartile range, IQR). The vertical lines (whiskers) show minimum and maximum values, excluding outliers. Outliers are defined as data points lying further than 1.5 times the IQR outside the box and are shown by empty circles. The MUE of monovalent lanthanide compounds with def2-SVPD basis sets is 4.1%, that of divalent lanthanide compounds is 4.4%, and that of tri- and tetravalent lanthanide compounds is 3.2%, similar to each other and well within the target accuracy, see Fig. 2(b)–(d). However, the MUE for def2-SVPD basis sets in neutral lanthanide dimers in Fig. 2(a) is much larger, with 10.0 % on average and the largest deviation of 18.8% found in Gd_2. Similarly, for def2-TZVPPD basis sets the overall MUE is 1.9%. Within this average statistic, basis set convergence is essentially reached for the tri- and tetravalent lanthanide compounds, which are only 0.4% away from the basis set limit. The MUEs for monovalent and divalent lanthanide compounds with def2-TZVPPD basis sets are 1.4% and 1.9%, respectively. At the same time, the zero-valent lanthanide compounds still have an unacceptably high 8.4% MUE with these basis sets. The overall MUE for def2-QZVPPD basis sets is 0.9%. This average encompasses the 3.3% MUE for zero-valent, 1.0% MUE for monovalent, 0.9% MUE for divalent, and a negligible 0.1% MUE for tri- and tetravalent lanthanide compounds. Note that the MUE for zero-valent compounds with def2-QZVPPD basis sets is again outside of the target accuracy. The complete results are shown in the Section S4 of the SM.

The MUE of atomic calculations is 8.0% with def2-SVPD basis sets (see Table II), just at the threshold of the target accuracy, even though we should keep in mind the considerable differences in basis set convergence between $4f^n5d^1$ and $4f^{n+1}$ states, as discussed above. The MUEs of atomic calculations with def2-TZVPPD and def2-QZVPPD basis sets are outside the target accuracy. Therefore, we define the extended def2-TZVPPDD and def2-QZVPPDD basis sets specifically for accurate calculations of lanthanide atoms and neutral metal clusters. In these basis sets, the diffuse augmentation is increased to 1p1d1f for the elements Ce–Nd and Gd–Tm. 1d1f diffuse set is used in def2-TZVPPDD basis sets for Pm–Sm and Er–Tm, while the larger 1p1d1f augmentation is needed in def2-QZVPPDD basis sets for these elements. In addition, 1p augmentation is included in the Eu def2-TZVPPDD basis set, and 1f diffuse set is used in the extended augmentation for Lu. With these additions, the MUE in atomic polarizabilities is 2.3% with def2-TZVPPDD basis sets.

The MUE for zero-valent lanthanide compounds is 2.1% with def2-TZVPPDD basis sets, compared to 8.4% for def2-TZVPPD. Both these values are within the 2.5% target accuracy for augmented triple-zeta valence basis sets. The def2-QZVPPDD basis sets produce results very close to the basis set limit: 0.2% MUE for lanthanide atoms, and 0.4% for zero-valent lanthanide compounds. The influence of the additional augmentation is quite small in the compounds of lanthanides in positive oxidation states, see Fig. 2. The extended basis sets are thus not necessary in these cases.

The property-optimized basis sets are included in the SM and are available from the Basis Set Exchange online service.[76,77]

TABLE I. Augmentation patterns of property-optimized basis sets for Ce–Lu.

	Augmentation		
	SVPD	TZVPPD	QZVPPD
Ce–Pr	1d1f	1d1f	1d1f
Nd–Sm, Gd–Tm	1d	1d	1d
Eu, Yb	–	–	1p
Lu	–	–	–

	Augmentation	
	TZVPPDD	QZVPPDD
Ce–Nd, Gd–Ho	1p1d1f	1p1d1f
Pm–Sm, Er–Tm	1d1f	1p1d1f
Eu	1p	1p
Yb	–	1p
Lu	1f	1f

TABLE II. Statistics of relative errors (in %) of static isotropic UHF polarizabilities α_{iso} of Ce–Yb atoms in their lowest $4f^n5d^1$ and $4f^{n+1}$ states (except Tm $4f^{12}5d^1$).

	SVP	SVPD	TZVPP	TZVPPD	TZVPPDD	QZVPP	QZVPPD	QZVPPDD
Mean	−12.9	−7.9	−8.3	−4.4	−0.5	−4.8	−3.1	−0.2
Mean uns.	12.2	8.0	8.3	4.6	2.3	4.8	3.1	0.2
Max neg.	−27.7	−22.5	−17.6	−11.1	−3.9	−8.7	−6.9	−0.9
Max pos.	0.5	0.6	...	1.9	12.2	...	0.0	0.1

TABLE III. Statistics of relative errors (in %) of static isotropic UHF polarizabilities α_{iso} of the molecular test set (70 molecules).

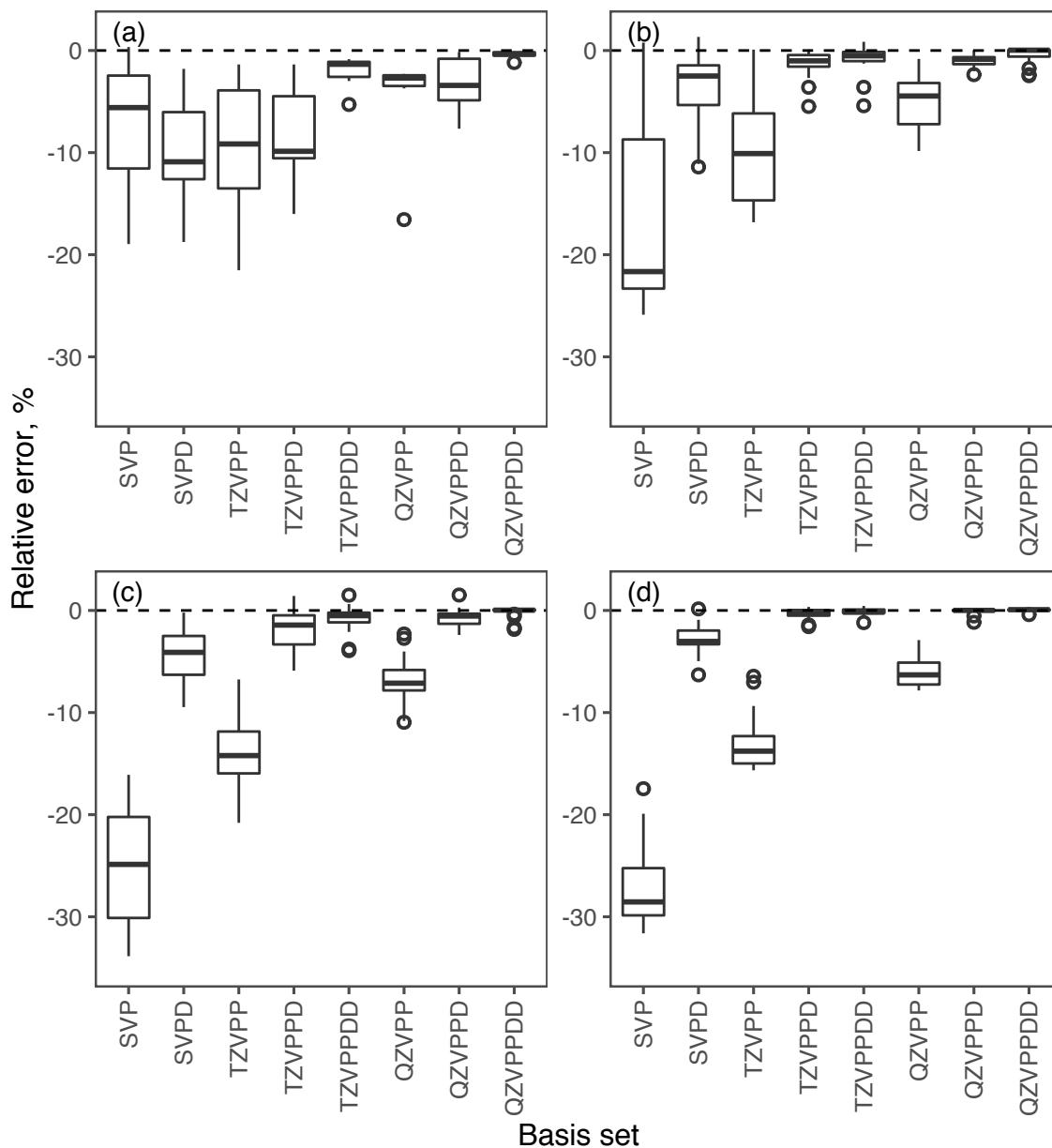|	SVP	SVPD	TZVPP	TZVPPD	TZVPPDD	QZVPP	QZVPPD	QZVPPDD
Mean	−22.6	−4.1	−12.4	−1.8	−0.7	−6.1	−0.8	−0.2
Mean uns.	22.6	4.4	12.4	1.9	0.9	6.1	0.9	0.3
Max neg.	−51.5	−18.8	−21.5	−16.0	−5.4	−16.6	−7.7	−2.5
	DyF	Gd_2	Gd_2	Gd_2	EuCl	Gd_2	Gd_2	ErF
Max pos.	0.8	9.2	0.1	1.4	1.5	...	1.5	0.2
	GdF	TbO_2	Lu_2N	DyO	DyO	...	$ErCl_2$	TbH_3

FIG. 2. Summary of relative errors (in %) of static isotropic UHF polarizabilities α_{iso} of (a) zero-valent lanthanide compounds (6 molecules), (b) monovalent lanthanide compounds (16 molecules), (c) divalent lanthanide compounds (27 molecules), and (d) tri- and tetravalent lanthanide compounds (21 molecules). The median error within each group is shown by a thick horizontal line, while the box covers the interquartile range between the first and third quartiles. The vertical lines (whiskers) show minimum and maximum values, excluding outliers. Outliers are shown by empty circles.

IV. APPLICATIONS TO LOW-VALENT LANTHANIDE COMPLEXES

The chemistry of lanthanide complexes in the +2 oxidation state, which was previously limited to Eu, Yb, and Sm, has been increasingly extended to other lanthanides.[40,78–80] One of the most complete series of low-valent lanthanide complexes is $LnCp_3'^-$ ($Cp' = C_5H_4SiMe_3$), which have been characterized for all lanthanides (except for radioactive Pm).[38–40,81] DFT studies showed that in the non-traditional $LnCp_3'^-$ complexes (Ln = Ce–Nd, Gd–Er) the highest occupied molecular orbitals (HOMOs) have d_{z^2} character, while the traditional complexes (in the sense of being part of better-known +2 chemistry, Ln = Sm–Eu, Tm–Yb) contain lanthanide +2 ions in their $4f^{n+1}$ configurations. The $4f^{n+1}$ and $4f^n5d^1$ configurations are close in energy in the Ln = Nd and Dy complexes, however these complexes were assigned $4f^n5d^1$ configurations on the basis of their x-ray crystal structures and electronic absorption spectra.[39] The differences in Ln–(Cp') centroid distances between the $LnCp_3'^-$ complexes and their $LnCp_3'$ precursors, which contain +3 lanthanides, was found to be small (0.02–0.04 Å) when the Ln^{+2} ions were in $4f^n5d^1$ configurations and usually larger (0.05–0.2 Å) for the Ln^{+2} ions with $4f^{n+1}$ configurations.[38–40,81] Moreover, complexes with $4f^n5d^1$ configurations show broad absorption bands in the UV/VIS range, in contrast to weaker and sharper electronic transitions typical of $4f^{n+1}$ configurations of +2 and +3 lanthanides.

The $LnCp_3'^-$ complexes provide a robust test set for the property-optimized basis sets due to the competition of the $4f^{n+1}$ and $4f^n5d^1$ configurations within the same series and its experimentally visible effects. We examine the basis set dependence of electronic excitations and UV/VIS absorption spectra of $LnCp_3'^-$ complexes with Ln = Ce–Nd, Sm[38,39] using time-dependent DFT (TDDFT). Of these four complexes, the ones with Ln = Ce–Pr have $4f^n5d^1$ configurations ($n = 1 - 2$), the Sm complex has a $4f^{n+1}$ configuration ($n = 5$), while the Nd complex is close to the configuration crossover point, with experimental data supporting the $4f^n5d^1$ configuration ($n = 3$).[39] The optimized ground-state structures of the Ln = Pr–Nd, Sm complexes were obtained from Refs. 38 and 39. For Ln = Ce, the anion geometry was extracted from the x-ray structure[39] (after removing counterions) and re-optimized with DFT using TPSSh hybrid functional[82], small-core ECPs,[32] and def2-SVP basis sets.[30,31] The average distance Ce–(Cp') centroid distance in the optimized structure was 2.56 Å, effectively unchanged from the experimental distance.[39] The RI-J approximation and optimized auxiliary basis sets were used throughout.[83,84] The effect of solution in THF

was approximated by the COSMO implicit solvent model[85] with dielectric constant $\epsilon = 7.52$. The optimized structure was confirmed to be an energy minimum by force constant calculations.[86,87]

TDDFT calculations of electronic excitation spectra[88–90] were performed at the optimized structures of the LnCp′$_3^-$ complexes (Ln = Ce–Nd, Sm) with the PBE0 hybrid functional[91]. We used the unaugmented def2-SVP and def2-TZVP basis sets as well as property-optimized def2-SVPD and def2-TZVPD basis sets. The latter was obtained by adding the diffuse augmentation of the def2-TZVPPD basis set to the smaller def2-TZVP basis sets. The oscillator strengths of electronic transitions were computed in the length gauge. COSMO corrections with the optical index of refraction $n = 1.405$ for THF were included in the response calculation. The spectral shapes were simulated from the resulting stick spectrum by empirical Gaussian broadening with 0.2 eV linewidth. The results are presented in Fig. 3. For reference, experimental spectra from Refs. 38 and 39 are shown. The complete results are given in the Section S6 of the SM.

As observed experimentally, the UV/VIS absorption spectra of LnCp′$_3^-$ complexes (Ln = Ce–Nd) containing lanthanide +2 ions in their 4f^{n}5d^1 configurations are dominated by intense transitions from the HOMO orbital, which has Ln 5d$_{z^2}$ character.[38–40,81] The experimental UV/VIS spectrum of the CeCp′$_3^-$ complex shows three major absorption bands at 635 nm, 540 nm, and 385 nm with a possible shoulder around 800 nm, see Fig. 3(a).[39] TDDFT results using def2-SVP basis sets miss the lower-energy features and contain two absorption bands at 759 nm and around 440 nm, respectively. Additional spectral features appear with def2-SVPD basis sets, with an absorption at 566 nm, which can be tentatively assigned to the experimental band at 540 nm. The main spectral features are qualitatively unchanged with triple-zeta basis sets, which have diffuse augmentation on Ce atom (denoted as TZVP(D) in Fig. 3), however the excitation energies are blue-shifted relative to def2-SVPD results. The lowest-energy band at ca. 760 nm in the spectrum of the CeCp′$_3^-$ complex is due to Laporte-allowed Ce d → f transitions, while the higher-energy transitions consist of combinations of Ce d → f and metal–ligand charge–transfer (MLCT) transitions into Cp′ π* orbitals. The spectral shape of the CeCp′$_3^-$ UV/VIS absorption spectrum is well reproduced with augmented double- and triple-zeta basis sets, however, the experimental excitation energies are somewhat overestimated, most likely due to method errors of the PBE0 functional and COSMO implicit solvation.
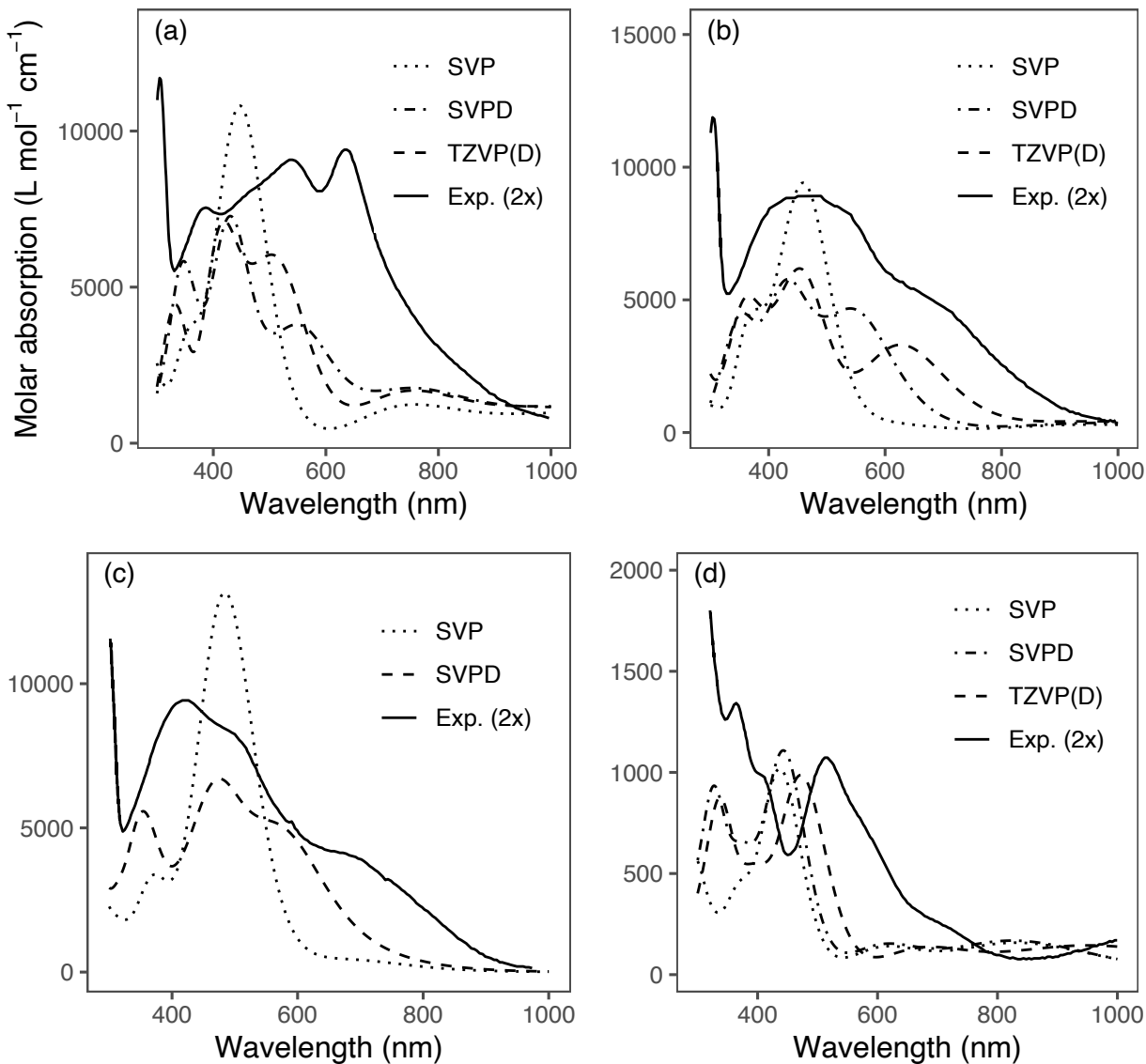
FIG. 3. Experimental and computed UV/VIS absorption spectra of LnCp$'^-_3$ complexes with Ln = (a) Ce, (b) Pr, (c) Nd, (d) Sm in THF. The experimental spectra are scaled 2x for clarity. See text for details.

The PrCp$'^-_3$ complex shows an absorption band at ca. 700 nm and a broad absorption peak between 410–540 nm in the experiment, see Fig. 3(b).[38] As for Ce, the lowest-energy absorption band is absent in the TDDFT results with def2-SVP basis sets and appears only upon augmentation. The TZVP(D) results are in good agreement with the experimental absorption spectra, apart from a blue-shift by ca. 0.15 eV. The 700 nm absorption band is assigned to transitions from Pr d into vacant Pr p orbitals. The broad absorption at higher

energies arises from transitions from the Pr d orbital into Pr f, Cp$'$ π^* and Rydberg orbitals.

The borderline NdCp$'_3^-$ complex exists in both $4f^3 5d^1$ and $4f^4$ configuration, the latter being more stable by merely 7 kcal/mol at the def2-SVP level. Consistent with Ref. 39, the predicted absorption spectrum of the higher-lying $4f^3 5d^1$ has higher intensity and is in better agreement with the experiment. However, this state becomes unstable with def2-TZVP basis sets, with or without augmentation. The results for the def2-SVP and def2-SVPD basis sets are shown in Fig. 3(c). The experimental absorption spectrum features three bands at 700 nm, 510 nm, and 420 nm. As with the neighboring LnCp$'_3^-$ complexes (Ln = Ce–Pr), the low-energy band is absent with def2-SVP basis sets. The def2-SVPD calculation predicts three main bands in good agreement with experiment. The low-energy absorption consists of Nd d $\rightarrow$ p transitions, while the higher-energy bands have MLCT character.

The absorption spectrum of the SmCp$'_3^-$ complex is much lower in intensity, which is typical of the complexes with the $4f^{n+1}$ configuration, as shown in Fig. 3(d).[39] As expected from our small-molecule results, the basis set effects are considerably smaller for this complex due to lack of the highly polarizable 5d orbital. The two experimental absorption bands at 515 nm and 410 nm are well reproduced already at the def2-SVP level. Augmentation does not change the qualitative spectral shape below 400 nm, while the extension to TZVP(D) basis sets results in a small red shift of the lower-energy band. The weak absorptions in the SmCp$'_3^-$ complex arise from Sm f $\rightarrow$ d transitions with additional MLCT contributions, as expected from absorption data of divalent lanthanides in crystals.[92]

V.   DISCUSSION

The basis set requirements of response properties of lanthanides and their compounds turn out to be both more element- and oxidation state-dependent than those in main-group elements and transition metals.[37] However, most of the observed trends can be understood in terms of the competing 4f and 5d occupations. The linear response of an orbital with angular momentum quantum number l to an electric dipole perturbation corresponds to $(l+1)$ and $(l-1)$ quantum numbers (the latter only for $l > 0$).[93] The 6s, 5d, and 4f subshells are energetically close in lanthanides, however, their spatial extent decreases significantly in the order 6s $\gg$ 5d $\gg$ 4f.[4,6] The 1p diffuse augmentation obtained by optimizing $4f^{n+1}$ reference states thus reflects the orbital response of the 6s valence orbitals and does not translate into

improved basis set convergence of lanthanide compounds, in which 6s orbitals are typically vacant. On the other hand, diffuse augmentation optimized using $4f^n5d^1$ reference states is determined by the lanthanide 5d orbitals. The largest improvements in atomic polarizabilities are from 1d diffuse augmentation, which corrects the description of the outlying part of the 5d orbitals. Further augmentation by 1f and 1p diffuse basis functions captures the response of the lanthanide 5d and 6s orbitals. The occupation and the spatial extent of the 5d orbitals are the determining factors for the basis set convergence of polarizabilities in lanthanide compounds. While the trivalent and tetravalent lanthanide compounds require little to no diffuse augmentation on the lanthanide atoms, diffuse basis functions are absolutely crucial for low-valent small molecules and organometallic complexes of lanthanides. The basis set requirements of property calculations in these groups of compounds are well covered by the default property-optimized def2-SVPD, def2-TZVPPD, and def2-QZVPPD basis sets. Therefore, the extended basis sets def2-TZVPPDD and def2-QZVPPDD should only be needed for a relatively narrow class of accurate calculations involving lanthanide atoms or neutral clusters.

Electron correlation and relativistic effects play an important role in polarizabilities of lanthanide atoms.[94,95] The basis set optimizations presented in this work are based on (unrestricted) HF with relativistic ECPs[32] and thus neglect electron correlation completely while treating relativistic effects at the scalar-relativistic level only. Thierfelder and Schwerdtfeger showed that scalar-relativistic effects at the DK2 level reduce the polarizability of the Yb ^1S state from the non-relativistic HF value of $\alpha_{\mathrm{iso}} = 230.1$ a. u. to 179.8 a. u. with DK2-HF,[94] primarily due to the contraction of the $6s^2$ subshell. Our HF basis set limit estimate of $\alpha_{\mathrm{iso}} = 190.4$ a. u. for Yb indicates that scalar-relativistic effects are only partially captured by the relativistic ECP. Electron correlation is another possible source of errors in polarizability calculations of lanthanide compounds. The inclusion of electron correlation at the non-relativistic CCSD(T) level reduces the polarizability of the Yb ^1S state by additional 40.9 a.u.[94] The effect of electron correlation thus seems to be much more significant in the Yb atom compared to main-group compounds, which showed only a 3.9% error for static HF polarizability calculations compared to CCSD(T) reference results in a recent benchmark of 145 carbon-containing molecules.[96] On average, our HF basis set limit estimates for Ce–Yb (excluding Lu due to ground-state stability issues) overshoot the best-estimate literature values[95] by 32%.

As the example of $LnCp'^-_3$ complexes (Ln = Ce–Nd, Sm) shows, 5d occupation is far from rare in low-valent lanthanide compounds. The response of the occupied d_{z^2} orbitals gives rise to novel optical[38–40,66,81] and magnetic[65,67,97,98] properties. Diffuse augmentation on lanthanide atoms is essential for accurate modeling of these properties. The augmented def2-SVPD, def2-TZVPPD, and def2-QZVPPD basis sets are well suited for this task. Interestingly, the UV/VIS absorption spectra of some $LnCp'^-_3$ complexes feature relatively intense Ln d → p transitions, as discussed in Section IV and the Section S6 of the SM. In all complexes studied in this work, the experimental absorption spectra were well reproduced without addition of diffuse p functions, which make only a minor contribution to the response of atomic $4f^n5d^1$ states, as can be seen from Fig. 1.

Although the property-optimized basis sets were developed by considering atomic polarizabilities at the HF level, they also perform very well for other molecular properties, for example, nonbonding interaction energies, electron affinities, and ground- and exited-state dipole moments, using HF, DFT, and correlated methods.[99] Due to the balanced construction of the property-optimized basis sets for lanthanides, we expect them to have a similar breadth of applications.

VI. CONCLUSIONS

We have developed property-optimized basis sets for the lanthanides Ce–Lu for use with small-core ECPs. Contrary to their reputation, these elements show an enormous variety in their response properties as a function of their oxidation state and 5d occupation. The default augmented basis sets for lanthanides balance the accuracy across the various bonding situations and provide $\leq 8\%$ accuracy with def2-SVPD basis sets, $\leq 2.5\%$ with def2-TZVPPD basis sets, and $\leq 1\%$ for def2-QZVPPD basis sets on the molecular test set, while keeping the size of the diffuse augmentation small. For accurate calculations of lanthanide atoms and neutral clusters, the default augmented basis sets are insufficient. The extended def2-TZVPPDD and def2-QZVPPDD basis sets include additional diffuse augmentations and are recommended for these applications.

SUPPLEMENTARY MATERIAL

See the supplementary material for UHF energies and static isotropic polarizabilities and of the molecular test set, Cartesian coordinates of the molecular test set, and electronic excitations in $LnCp_3'^-$ complexes ($Cp' = C_5H_4SiMe_3$, Ln = Ce–Nd, Sm).

ACKNOWLEDGMENTS

DATA AVAILABILITY

The data that support the findings of this study are available within the article and its supplementary material.

REFERENCES

[1] L. Brewer, "Systematics and the properties of the lanthanides," in *Systematics and the Properties of the Lanthanides*, edited by S. P. Sinha (Springer, Dordrecht, 1983) pp. 17–69.

[2] J. E. Sansonetti and W. C. Martin, "Handbook of basic atomic spectroscopic data," J. Phys. Chem. Ref. Data **34**, 1559–2259 (2005).

[3] K. Balasubramanian, "Relativistic effects and electronic structure of lanthanide and actinide molecules," in *Handbook on the Physics and Chemistry of Rare Earths*, Vol. 18, edited by K. A. Gschneidner, Jr., L. Eyring, G. R. Choppin, and G. H. Lander (Elsevier, Amsterdam, 1994) Chap. 119, pp. 29–158.

[4] M. Dolg and H. Stoll, "Electronic structure calculations for molecules containing lanthanide atoms," in *Handbook on the Physics and Chemistry of Rare Earths*, Vol. 22, edited by K. A. Gschneidner, Jr. and L. Eyring (Elsevier, Amsterdam, 1996) Chap. 152, pp. 607–729.

[5]M. Dolg, ed., *Computational Methods in Lanthanide and Actinide Chemistry* (Wiley, Chichester, 2018).

[6]K. A. Peterson and K. G. Dyall, "Gaussian basis sets for lanthanide and actinide elements: Strategies for their development and use," in *Computational Methods in Lanthanide and Actinide Chemistry*, edited by M. Dolg (Wiley, Chichester, 2015) Chap. 8, pp. 195–216.

[7]F. Weigend, "Error-balanced segmented contracted Gaussian basis sets. A concept and its extension to the lanthanides," in *Computational Methods in Lanthanide and Actinide Chemistry*, edited by M. Dolg (Wiley, Chichester, 2015) Chap. 7, pp. 181–194.

[8]K. A. Peterson and J. G. Hill, "On the development of accurate Gaussian basis sets for f-block elements," Annu. Rep. Comput. Chem. **14**, 47–74 (2018).

[9]T. Tsuchiya, M. Abe, T. Nakajima, and K. Hirao, "Accurate relativistic Gaussian basis sets for H through Lr determined by atomic self-consistent field calculations with the third-order Douglas–Kroll approximation," J. Chem. Phys. **115**, 4463–4472 (2001).

[10]T. Nakajima and K. Hirao, "Accurate relativistic Gaussian basis sets determined by the third-order Douglas–Kroll approximation with a finite-nucleus model," J. Chem. Phys. **116**, 8270 (2002).

[11]B. O. Roos, R. Lindh, P.-Å. Malmqvist, V. Veryazov, P.-O. Widmark, and A. C. Borin, "New relativistic atomic natural orbital basis sets for lanthanide atoms with applications to the Ce diatom and LuF_3," J. Phys. Chem. A **112**, 11431–11435 (2008).

[12]D. A. Pantazis and F. Neese, "All-electron scalar relativistic basis sets for the lanthanides," J. Chem. Theory Comput. **5**, 2229–2238 (2009).

[13]D. Aravena, F. Neese, and D. A. Pantazis, "Improved segmented all-electron relativistically contracted basis sets for the lanthanides," J. Chem. Theory Comput. **12**, 1148–1156 (2016).

[14]M. Dolg, "Segmented contracted Douglas–Kroll–Hess adapted basis sets for lanthanides," J. Chem. Theory Comput. **7**, 3131–3142 (2011).

[15]M. Sekiya, T. Noro, T. Koga, and T. Shimazaki, "Relativistic segmented contraction basis sets with core-valence correlation effects for atoms $_{57}$La through $_{71}$Lu: Sapporo-DK-nZP sets (n = D, T, Q)," Theor. Chem. Acc. **131**, 1247 (2012).

[16]Q. Lu and K. A. Peterson, "Correlation consistent basis sets for lanthanides: The atoms La–Lu," J. Chem. Phys. **145**, 054111 (2016).

[17]F. E. Jorge, L. S. C. Martins, and M. L. Franco, "All-electron double zeta basis sets for the lanthanides: Application in atomic and molecular property calculations," Chem. Phys.

Lett. **643**, 84–88 (2016).

[18] A. Z. de Oliveira, I. B. Ferreira, C. T. Campos, F. E. Jorge, and P. A. Fantin, "Segmented all-electron basis sets of triple zeta quality for the lanthanides: Application to structure calculations of lanthanide monoxides," J. Mol. Model. **25**, 38 (2019).

[19] I. B. Ferreira, C. T. Campos, and F. E. Jorge, "All-electron basis sets augmented with diffuse functions for He, Ca, Sr, Ba, and lanthanides: Application in calculations of atomic and molecular properties," J. Mol. Model. **26**, 95 (2020).

[20] A. S. P. Gomes, K. G. Dyall, and L. Visscher, "Relativistic double-zeta, triple-zeta, and quadruple-zeta basis sets for the lanthanides La–Lu," Theor. Chem. Acc. **127**, 369–381 (2010).

[21] J. P. Zobel, P.-O. Widmark, and V. Veryazov, "The ANO-R basis set," J. Chem. Theory Comput. **16**, 278–294 (2020).

[22] P. Pollak and F. Weigend, "Segmented contracted error-consistent basis sets of double- and triple-ζ valence quality for one- and two-component relativistic all-electron calculations," J. Chem. Theory Comput. **13**, 3696–3705 (2017).

[23] Y. J. Franzke, L. Spiske, P. Pollak, and F. Weigend, "Segmented contracted error-consistent basis sets of quadruple-ζ valence quality for one- and two-component relativistic all-electron calculations," J. Chem. Theory Comput. **16**, 5658–5674 (2020).

[24] T. R. Cundari and W. J. Stevens, "Effective core potential methods for the lanthanides," J. Chem. Phys. **98**, 5555–5565 (1993).

[25] R. B. Ross, S. Gayen, and W. C. Ermler, "Ab initio relativistic effective potentials with spin–orbit operators. V. Ce through Lu," J. Chem. Phys. **100**, 8145–8155 (1994).

[26] M. Hülsen, A. Weigand, and M. Dolg, "Quasirelativistic energy-consistent 4f-in-core pseudopotentials for tetravalent lanthanide elements," Theor. Chem. Acc. **122**, 23–29 (2009).

[27] M. Hülsen, M. Dolg, P. Link, and U. Ruschewitz, "Improved valence basis sets for divalent lanthanide 4f-in-core pseudopotentials," Theor. Chem. Acc. **129**, 367–379 (2011).

[28] X. Cao and M. Dolg, "Valence basis sets for relativistic energy-consistent small-core lanthanide pseudopotentials," J. Chem. Phys. **115**, 7348–7355 (2001).

[29] X. Cao and M. Dolg, "Segmented contraction scheme for small-core lanthanide pseudopotential basis sets," J. Mol. Struct. THEOCHEM **581**, 139–147 (2002).

[30] R. Gulde, P. Pollak, and F. Weigend, "Error-balanced segmented contracted basis sets of Double-ζ to Quadruple-ζ valence quality for the lanthanides," J. Chem. Theory Comput.

8, 4062–4068 (2012).

[31] F. Weigend and R. Ahlrichs, "Balanced basis sets of split valence, triple zeta valence and quadruple zeta valence quality for H to Rn: Design and assessment of accuracy," Phys. Chem. Chem. Phys. **7**, 3297–3305 (2005).

[32] M. Dolg, H. Stoll, and H. Preuss, "Energy adjusted *ab initio* pseudopotentials for the rare earth elements," J. Chem. Phys. **90**, 1730–1734 (1989).

[33] J. G. Hill, "Gaussian basis sets for molecular applications," Int. J. Quant. Chem. **113**, 21–34 (2013).

[34] F. Jensen, "Atomic orbital basis sets," WIREs Comput. Mol. Sci. **3**, 273–295 (2013).

[35] B. Nagy and F. Jensen, "Basis sets in quantum chemistry," in *Reviews in Computational Chemistry*, Vol. 30, edited by A. L. Parrill and K. B. Lipkowitz (Wiley, Hoboken NJ, 2018) Chap. 3, pp. 93–149.

[36] A. A. Buchachenko, G. Chałasiński, and M. M. Szcześniak, "Diffuse basis functions for small-core relativistic pseudopotential basis sets and static dipole polarizabilities of selected lanthanides La, Sm, Eu, Tm and Yb," Struct. Chem. **18**, 769–772 (2007).

[37] D. Rappoport and F. Furche, "Property-optimized Gaussian basis sets for molecular response calculations," J. Chem. Phys. **133**, 134105 (2010).

[38] M. R. MacDonald, J. E. Bates, J. W. Ziller, F. Furche, and W. J. Evans, "Completing the series of +2 ions for the lanthanide elements: Synthesis of molecular complexes of Pr^{2+}, Gd^{2+}, Tb^{2+}, and Lu^{2+}," J. Am. Chem. Soc. **135**, 9857–9868 (2013).

[39] M. E. Fieser, M. R. MacDonald, B. T. Krull, J. E. Bates, J. W. Ziller, F. Furche, and W. J. Evans, "Structural, spectroscopic, and theoretical comparison of traditional vs recently discovered Ln^{2+} ions in the $[K(2.2.2\text{-cryptand})][(C_5H_4SiMe_3)_3Ln]$ complexes: The variable nature of Dy^{2+} and Nd^{2+}," J. Am. Chem. Soc. **137**, 369–382 (2015).

[40] D. H. Woen and W. J. Evans, "Expanding the +2 oxidation state of the rare-earth metals, uranium, and thorium in molecular complexes," in *Handbook on the Physics and Chemistry of Rare Earths*, Vol. 50, edited by J.-C. G. B. K. A. Gschneidner, Jr. and V. K. Pecharsky (Elsevier, Amsterdam, 2016) pp. 337–394.

[41] J. O. Hirschfelder, W. Byers Brown, and S. T. Epstein, "Recent developments in perturbation theory," in *Advances in Quantum Chemistry*, Vol. 1, edited by P.-O. Löwdin (Academic Press, New York, 1964) pp. 255–374.

[42]E. A. Hylleraas, "Über den Grundterm der Zweielektronenprobleme von H$^-$, He, Li$^+$, Be^{++} usw." Z. Phys. **65**, 209–225 (1930).

[43]R. Jurgens-Lutovsky and J. Almlöf, "Dual basis sets in calculations of electron correlation," Chem. Phys. Lett. **178**, 451–454 (1991).

[44]L. Maschio and B. Kirtman, "Coupled perturbation theory approach to dual basis sets for molecules and solids. 1. General theory and application to molecules," J. Chem. Theory Comput. **16**, 340–353 (2019).

[45]D. Rappoport, "Basis-set quality and basis-set bias in molecular property calculations," ChemPhysChem **12**, 3404–3413 (2011).

[46]F. Furche, B. T. Krull, B. D. Nguyen, and J. Kwon, "Accelerating molecular property calculations with nonorthonormal Krylov space methods," J. Chem. Phys. **144**, 174105 (2016).

[47]J. Čížek and J. Paldus, "Stability conditions for the solutions of the Hartree–Fock equations for atomic and molecular systems. application to the Pi-electron model of cyclic polyenes," J. Chem. Phys. **47**, 3976–3985 (1967).

[48]D. J. Thouless, "Stability conditions and nuclear rotations in the Hartree–Fock theory," Nucl. Phys. **21**, 225–232 (1960).

[49]R. Bauernschmitt and R. Ahlrichs, "Stability analysis for solutions of the closed shell Kohn–Sham equation," J. Chem. Phys. **104**, 9047–9052 (1996).

[50]A. D. Becke, "Density-functional exchange-energy approximation with correct asymptotic behavior," Phys. Rev. A **38**, 3098–3100 (1988).

[51]J. P. Perdew, "Density-functional approximation for the correlation energy of the inhomogeneous electron gas," Phys. Rev. B **33**, 8822–8824 (1986).

[52]F. Weigend, F. Furche, and R. Ahlrichs, "Gaussian basis sets of quadruple zeta valence quality for atoms H–Kr," J. Chem. Phys. **119**, 12753–12762 (2003).

[53]A. E. Reed, R. B. Weinstock, and F. Weinhold, "Natural population analysis," J. Chem. Phys. **83**, 735–746 (1985).

[54]S. G. Balasubramani, G. P. Chen, S. Coriani, M. Diedenhofen, M. S. Frank, Y. J. Franzke, F. Furche, R. Grotjahn, M. E. Harding, C. Hättig, A. Hellweg, B. Helmich-Paris, C. Holzer, U. Huniar, M. Kaupp, A. M. Khah, S. K. Khani, T. Müller, F. Mack, B. D. Nguyen, S. M. Parker, E. Perlt, D. Rappoport, K. Reiter, S. Roy, M. Rückert, G. Schmitz, M. Sierka, E. Tapavicza, D. P. Tew, C. van Wüllen, V. K. Voora, F. Weigend, A. Wodyński, and

J. M. Yu, "TURBOMOLE: Modular program suite for ab initio quantum-chemical and condensed-matter simulations," J. Chem. Phys. **152**, 184107 (2020).

[55]TURBOMOLE V7.5 2020, a development of University of Karlsruhe and Forschungszentrum Karlsruhe GmbH, 1989-2007, TURBOMOLE GmbH, since 2007; available from https://www.turbomole.org.

[56]M. Dolg, H. Stoll, and H. Preuss, "Homonuclear diatomic lanthanoid compounds: a pseudopotential configuration interaction and correlation energy density functional study," J. Mol. Struct. THEOCHEM **277**, 239–249 (1992).

[57]X. Cao and M. Dolg, "Electronic structure of lanthanide dimers," Mol. Phys. **101**, 1967–1976 (2003).

[58]J. R. Lombardi and B. Davis, "Periodic properties of force constants of small transition-metal and lanthanide clusters," Chem. Rev. **102**, 2431–2460 (2002).

[59]J. O. Kafader, J. E. Topolski, and C. C. Jarrold, "Molecular and electronic structures of cerium and cerium suboxide clusters," J. Chem. Phys. **145**, 154306 (2016).

[60]B. Roos and P. Pyykkö, "Bonding trends in molecular compounds of lanthanides: The double-bonded carbene cations $LnCH_2^+$ (Ln=Sc, Y, La–Lu)," Chem. Eur. J. **16**, 270–275 (2010).

[61]W. Xu, X. Jin, M. Chen, P. Pyykkö, M. Zhou, and J. Li, "Rare-earth monocarbonyls MCO: comprehensive infrared observations and a transparent theoretical interpretation for M = Sc; Y; La–Lu," Chem. Sci. **3**, 1548–1554 (2012).

[62]F. G. N. Cloke, "Zero oxidation state compounds of scandium, yttrium, and the lanthanides," Chem. Soc. Rev. **22**, 17–24 (1993).

[63]G. B. Deacon and Q. Shen, "Complexes of lanthanoids with neutral π donor ligands," J. Organomet. Chem. **511**, 1–17 (1996).

[64]G. Hong, F. Schautz, and M. Dolg, "Ab initio study of metal–ring bonding in the bis(η^6-benzene)lanthanide and -actinide complexes $M(C_6H_6)_2$ (M = La, Ce, Nd, Gd, Tb, Lu, Th, U)," J. Am. Chem. Soc. **121**, 1502–1512 (1999).

[65]K. R. Meihaus, M. E. Fieser, J. F. Corbey, W. J. Evans, and J. R. Long, "Record high single-ion magnetic moments through $4f^n5d^1$ electron configurations in the divalent lanthanide complexes $[(C_5H_4SiMe_3)_3Ln]^-$," J. Am. Chem. Soc. **137**, 9855–9860 (2015).

[66]A. J. Ryan, L. E. Darago, S. G. Balasubramani, G. P. Chen, J. W. Ziller, F. Furche, J. R. Long, and W. J. Evans, "Synthesis, structure, and magnetism of tris(amide)

$[Ln\{N(SiMe_3)_2\}_3]^{1-}$ complexes of the non-traditional +2 lanthanide ions," Chem. Eur. J. **24**, 7702–7709 (2018).

[67] C. A. Gould, K. R. McClain, J. M. Yu, T. J. Groshens, F. Furche, B. G. Harvey, and J. R. Long, "Synthesis and magnetism of neutral, linear metallocene complexes of Terbium(II) and Dysprosium(II)," J. Am. Chem. Soc. **141**, 12967–12973 (2019).

[68] X. Shen, L. Fang, X. Chen, and J. R. Lombardi, "Absorption, excitation, and resonance raman spectra of Ce_2, Pr_2, and Nd_2," J. Chem. Phys. **113**, 2233–2237 (2000).

[69] M. Dolg, H. Stoll, and H. Preuss, "Pseudopotential study on rare earth dihalides and trihalides," J. Mol. Struct. THEOCHEM **235**, 67–79 (1991).

[70] T. R. Cundari, S. O. Sommerer, L. A. Strohecker, and L. Tippett, "Effective core potential studies of lanthanide complexes," J. Chem. Phys. **103**, 7058–7063 (1995).

[71] T. Tsuchiya, T. Taketsugu, H. Nakano, and K. Hirao, "Theoretical study of electronic and geometric structures of a series of lanthanide trihalides LnX_3 (Ln=La–Lu; X=Cl, F)," J. Mol. Struct. THEOCHEM **461**, 203–222 (1999).

[72] W. Xu, W.-X. Ji, Y.-X. Qiu, W. H. E. Schwarz, and S.-G. Wang, "On structure and bonding of lanthanoid trifluorides LnF_3 (Ln = La to Lu)," Phys. Chem. Chem. Phys. **15**, 7839–7847 (2013).

[73] Y. Wang and M. Dolg, "Pseudopotential study of the ground and excited states of Yb_2," Theor. Chem. Acc. **100**, 124–133 (1998).

[74] A. A. Buchachenko, G. Chałasiński, and M. M. Szcześniak, "Europium dimer: van der Waals molecule with extremely weak antiferromagnetic spin coupling," J. Chem. Phys. **131**, 241102 (2009).

[75] P. Schwerdtfeger, O. R. Smits, and P. Pyykkö, "The periodic table and the physics that drives it," Nat. Rev. Chem. **4**, 359–380 (2020).

[76] B. P. Pritchard, D. Altarawy, B. Didier, T. D. Gibson, and T. L. Windus, "New basis set exchange: An open, up-to-date resource for the molecular sciences community," J. Chem. Inf. Model. **59**, 4814–4820 (2019).

[77] Basis Set Exchange, developed as a collaboration between the Molecular Sciences Software Institute (MolSSI) and the Pacific Northwest National Lab/Environmental Molecular Sciences Laboratory (PNNL/EMSL), `https://www.basissetexchange.org`.

[78] M. N. Bochkarev, "Molecular compounds of "new" divalent lanthanides," Coord. Chem. Rev. **248**, 835–851 (2004).

[79]F. Nief, "Molecular chemistry of the rare-earth elements in uncommon low-valent states," in *Handbook on the Physics and Chemistry of Rare Earths*, Vol. 40, edited by K. A. Gschneidner, Jr., J.-C. G. Bünzli, and V. K. Pecharsky (Elsevier, Amsterdam, 2010) Chap. 246, pp. 241–300.

[80]R. Collins, J. P. Durrant, M. He, and R. A. Layfield, "Electronic structure and magnetic properties of rare-earth organometallic sandwich compounds," in *Handbook on the Physics and Chemistry of Rare Earths*, Vol. 55, edited by J.-C. G. Bünzli and V. K. Pecharsky (Elsevier, Amsterdam, 2019) Chap. 307, pp. 89–121.

[81]M. R. MacDonald, J. E. Bates, M. E. Fieser, J. W. Ziller, F. Furche, and W. J. Evans, "Expanding rare-earth oxidation state chemistry to molecular complexes of Holmium(II) and Erbium(II)," J. Am. Chem. Soc. **134**, 8420–8423 (2012).

[82]V. N. Staroverov, G. E. Scuseria, J. Tao, and J. P. Perdew, "Comparative assessment of a new nonempirical density functional: Molecules and hydrogen-bonded complexes," J. Chem. Phys. **119**, 12129–12137 (2003).

[83]K. Eichkorn, O. Treutler, H. Öhm, M. Häser, and R. Ahlrichs, "Auxiliary basis sets to approximate Coulomb potentials (Chem. Phys. Letters 240 (1995) 283-290)," Chem. Phys. Lett. **242**, 652–660 (1995).

[84]F. Weigend, "Accurate Coulomb-fitting basis sets for H to Rn," Phys. Chem. Chem. Phys. **8**, 1057–1065 (2006).

[85]A. Klamt and G. Schüürmann, "COSMO: a new approach to dielectric screening in solvents with explicit expressions for the screening energy and its gradient," J. Chem. Soc. Perkin Trans. 2 , 799–805 (1993).

[86]P. Deglmann, F. Furche, and R. Ahlrichs, "An efficient implementation of second analytical derivatives for density functional methods," Chem. Phys. Lett. **362**, 511–518 (2002).

[87]P. Deglmann, K. May, F. Furche, and R. Ahlrichs, "Nuclear second analytical derivative calculations using auxiliary basis set expansions," Chem. Phys. Lett. **384**, 103–107 (2004).

[88]R. Bauernschmitt and R. Ahlrichs, "Treatment of electronic excitations within the adiabatic approximation of time dependent density functional theory," Chem. Phys. Lett. **256**, 454–464 (1996).

[89]R. Bauernschmitt, M. Häser, O. Treutler, and R. Ahlrichs, "Calculation of excitation energies within time-dependent density functional theory using auxiliary basis set expansions," Chem. Phys. Lett. **264**, 573–578 (1997).

[90] F. Furche and D. Rappoport, "III. Density functional methods for excited states: Equilibrium structure and electronic spectra," in *Computational Photochemistry*, Vol. 16, edited by M. Olivucci (Elsevier, Amsterdam, 2005) pp. 93–128.

[91] J. P. Perdew, M. Ernzerhof, and K. Burke, "Rationale for mixing exact exchange with density functional approximations," J. Chem. Phys. **105**, 9982–9985 (1996).

[92] G. H. Diecke, H. M. Crosswhite, and H. Crosswhite, *Spectra and Energy Levels of Rare Earth Ions in Crystals* (Wiley-Interscience, New York, 1968).

[93] A. J. Sadlej, "Medium-size polarized basis sets for high-level correlated calculations of molecular electric properties," Coll. Czech. Chem. Commun. **53**, 1995–2016 (1988).

[94] C. Thierfelder and P. Schwerdtfeger, "Effect of relativity and electron correlation in static dipole polarizabilities of ytterbium and nobelium," Phys. Rev. A **79**, 032512 (2009).

[95] P. Schwerdtfeger and J. K. Nagle, "2018 Table of static dipole polarizabilities of the neutral elements in the periodic table," Mol. Phys. **117**, 1200–1225 (2018).

[96] T. Wu, Y. N. Kalugina, and A. J. Thakkar, "Choosing a density functional for static molecular polarizabilities," Chem. Phys. Lett. **635**, 257–261 (2015).

[97] V. Dubrovin, A. A. Popov, and S. Avdoshenko, "Magnetism in ln molecular systems with 4f/valence-shell interplay (FV-magnetism)," Chem. Commun. **55**, 13963–13966 (2019).

[98] V. E. Fleischauer, G. Ganguly, D. H. Woen, N. J. Wolford, W. J. Evans, J. Autschbach, and M. L. Neidig, "Insight into the electronic structure of formal lanthanide(II) complexes using magnetic circular dichroism spectroscopy," Organometallics **38**, 3124–3131 (2019).

[99] A. Hellweg and D. Rappoport, "Development of new auxiliary basis functions of the Karlsruhe segmented contracted basis sets including diffuse basis functions (def2-SVPD, def2-TZVPPD, and def2-QVPPD) for RI-MP2 and RI-CC calculations," Phys. Chem. Chem. Phys. **17**, 1010–1017 (2014).